THE PHOTOASSISTED DECARBOXYLATION OF ACETATE ON n-TYPE RUTILE ELECTRODES - THE PHOTO-KOLBE REACTION

Bernhard Kraeutler and Allen J. Bard*

Department of Chemistry, The University of Texas at Austin, Austin, TX 78712

Introduction

Intensive research on semiconductor electrode processes is currently mainly concerned with the conversion of light energy into electrical or chemical energy in photovoltaic and photoelectrosynthetic, liquid junction, solar cells, respectively.[1] The goal of finding an efficient, economic and durable photoelectrochemical system for solar energy conversion has led to a widespread search for optimal electrode and solution compositions in photoelectrochemical solar cells. A third application of semiconductor electrochemistry is photocatalysis[2] where light energy is used to drive a chemical transformation in a spontaneous direction and the invested radiant energy is not stored in some other, useful form, but is used to overcome the energy of activation needed to drive the reaction. This parallels some electrosynthetic processes where electrical energy helps to carry out a chemical reaction, often without producing a product with higher energy content (but with higher structural value). For example in the electrochemical Kolbe decarboxylation[3] of carboxylic acids, one of the most important synthetic electroorganic reactions, the overall cell process ($2\ RCO_2H \rightarrow R\text{-}R + 2\ CO_2 + H_2$) is exoenergetic for most simple carboxylic acids. We have previously described[4] preliminary experiments on the photoassisted Kolbe reaction of acetate on a single crystal n-type TiO_2 (rutile)

electrode in acetonitrile (ACN) solutions. The overall reaction at the illuminated anode was predominantly

$$2CH_3CO_2^- + 2h^+ \rightarrow C_2H_6 + CO_2 \quad (1)$$

and the rapid,[5] irreversible decarboxylation of the postulated intermediate acyloxy radicals provided an additional driving force for the overall reaction. On metal electrodes, the oxidation potentials necessary to initiate the electrochemical Kolbe reaction are generally very high (>2.2 V vs. S.C.E. on Pt in aqueous solutions of carboxylic acids).[3] Therefore, a wide band-gap n-type semiconductor n-TiO_2 (rutile, band-gap energy E_g = 3.02 ev[6]) was selected as electrode material. This choice was further encouraged by the high chemical stability of rutile (that inhibited photodecomposition of the semiconductor in the photoassisted decomposition of water[7,8]) and by the extensive knowledge on the behavior of rutile electrodes.[8,9] Finally, the as yet incomplete mechanistic picture of the electrochemical Kolbe reaction on metal electrodes[3] and the anticipated kinetic effect of a large band-gap semiconductor on follow-up electron transfer reactions were further points that spurred our interest in a photocatalyzed Kolbe reaction on n-type rutile electrodes.

The photooxidation of carboxylic acids has received only minor attention in the past,[10] and the addition of carboxylic acids to aqueous solutions were mainly used in attempts to stabilize n-type semiconductor electrodes against photodecomposition. We report here details of the photo-Kolbe reaction of acetate on rutile electrodes in ACN, acetic acid, and aqueous solutions, which leads to the efficient production of ethane.

Experimental Section

Materials. Acetonitrile (ACN, spectrograde, Matheson, Coleman & Bell) was dried and purified as previously described[11] and was stored under helium in a

glove box (Vacuum Atmospheres Corporation, Hawthorne, Calif.). Glacial acetic acid (HAc, Fischer) was recrystallized and stored under nitrogen at 0°C. Tetra-n-butylammonium acetate (TBBAAc) was prepared by mixing equimolar amounts of tetra-n-butylammonium hydroxide (titration-grade, 1.0M in methanol, Southwestern Analytical Chemicals Inc.) and glacial acetic acid, removal of solvent under vacuum at 60°C and drying of the remaining colorless solid at 10^{-4} Torr at room-temperature for 5 days. Tetra-n-butylammonium perchlorate (TBAP, polarographic grade), sodium perchlorate (reagent grade) and sodium acetate (reagent grade) were dried under vacuum (~10^{-4} Torr, 3 days, room-temperature) and stored under inert gas. Perchloric acid (Fisher, 70%) was used without further treatment.

The TiO_2 electrode was either a chemically vapor deposited polycrystalline electrode (Ti-substrate, area ca. 1 cm^2)[9f] or a single crystal rutile electrode. The single crystal electrodes were prepared by cutting a 1 mm slice from a larger crystal (Fuji Titanium, Hiratsuka, Japan) with a surface area of the 001 face of ~1 cm^2; it was doped at 600° under H_2 for 35 min and polished with 0.5 μm alumina. On the backside of the electrode an ohmic contact was made with Ga-In alloy to which a Cu-wire was attached with conducting silver epoxy (method d in ref. 12). The back of the electrode was then insulated with 5 min epoxy (Devcon Corp., Danvers, Mass.) and mounted on a flat piece of glass with the Cu-leads running through an attached glass tube. For work in ACN and HAc, the epoxy coating was covered with silicone adhesive (Dow-Corning, Midland, Mich.) leaving an exposed electrode surface area of ~0.5 cm^2. Before starting the experiments, the electrode was etched for 30 seconds in an HF-etching solution[9e,13] and carefully rinsed with distilled water, then air-dried.

Apparatus. A three-compartment cell[9e] served for the electroanalytical measurements, while for preparative runs a one-compartment cell with a flat

Pyrex window was used. The reference electrodes were a silver wire or a Ag/0.1 M $AgNO_3$ electrode for ACN (Potential: +0.34 V vs. SCE[14,15]); a saturated calomel electrode (SCE) for measurements in water, and a mercury/mercurous acetate electrode (Hg/Hg_2Ac_2 (saturated) in HAc/0.5 M $NaClO_4$ and 0.05 M NaAc)[16] for measurements with acetic acid as solvent. A coiled platinum wire was the counter electrode. A platinum disk electrode (area 5 mm^2) was also used as a working electrode for voltammetric measurements.

In all experiments air was kept out of the cell, either by working in the glove box, by using an air-tight system, or by constantly purging the main compartment with prepurified nigrogen. In several preparative runs, such a stream of nitrogen was used to carry the volatile reaction products out of the cell and into a saturated solution of $Ba(OH)_2$ in aq. 1 M NaOH, thus precipitating CO_2 quantitatively as $BaCO_3$.

The measurements were done with a PAR 173 potentiostat using positive feedback for cell resistances, a PAR 175 universal programmer and a PAR 179 digital coulometer (Princeton Applied Research Corporation, Princeton, N.J.) and were recorded on a Houston Instruments (Austin, Texas) Model 2000 X-Y recorder. The light source was a 450 W xenon lamp (Oriel Corp., Stamford, Conn.) using a model 6242 power supply. A grating monochromator (model 7240, Oriel Corp.) and an EG & G Model 550 radiometer (EG & G, Incorp., Salem, Mass.) served in wavelength and quantum yield studies. pH measurements were performed with a Beckmann "Expandomatic" pH-meter using a calibrated glass electrode.

Results

Acetate photooxidation in acetonitrile. Rutile electrodes have already been studied with respect to most electrochemical parameters in the aprotic

polar solvent/electrolyte system ACN/0.1 N TBAP.[9e] An aprotic solvent such as ACN offers a wide potential working range which facilitates electroanalytical and preparative investigations of photoelectrochemical reactions. Typical was the absence of dark oxidative currents (up to + 7 V vs. SCE) and the insignificance of reductive currents to potentials as negative as -2.8 V on doped rutile single crystal electrodes.[9e] Under full irradiation from the 450 W xenon lamp (slightly defocused to cover the exposed electrode surface) background photooxidation of dry ACN/0.1 N TBAP solutions on the rutile electrodes became significant at potentials positive of ~ +1 V vs. the Ag/0.1 N Ag/NO_3 electrode, reaching a limiting photocurrent of ~ 16 mA/cm^2 at potentials beyond +2 V.[4] A small, mass transfer controlled photooxidation wave at less positive potentials was presumably due to residual water, as addition of 1.5 vol.-% of water caused this wave to increase in size and reach the limiting background photocurrent. Similar results were recently also reported by Nakatani and Tsubomura.[17] The single crystal rutile electrode was found to be stable with respect to the photooxidative background processes. When a doped single crystal rutile electrode was illuminated with the 450 W xenon lamp and at an applied potential of +3 V vs. Ag/0.1 N $AgNO_3$ with 30.1 Coulombs (corresponding to 30.4 mmole) passed and the electrode then dismantled and cleaned, there was no loss of weight (131.0 mg before and 131.1 mg after the experiment) or any observable destruction of the electrode surface. The resistance of the solution components (ACN/0.1 M TBAP) against photooxidation as well as the high electrode stability thus allow a large potential span (~ 2 V free of background potooxidation currents) positive of the flat band potential V_{fb} (~-1.0 V vs. SCE[9e, 17]) for relatively uncomplicated photoelectrosynthesis on rutile electrodes. This is in sharp contrast to the behavior exhibited by illuminated rutile electrodes in aqueous solutions, where

V_{fb} and the onset of solvent oxidation practically coincide.

Addition of the soluble acetate salt, TBAAc, did not affect noticeably the dark currents in either the oxidative or reductive potential ranges. However, under illumination of the exposed electrode surface (with the full output of the 450 W xenon lamp) a new, broad photooxidation wave appeared (Fig. 1)[4]. The i-V curves measured at potential scan rates, v, of 0.05 to 0.5 V/sec showed that the onset of the acetate photooxidation was at ~-1.6 V vs. the Ag/0.1 N $AgNO_3$ reference (for 0.1 M TBAAc), a potential about 300 mV more negative than V_{fb} determined in ACN containing 0.1 M TBAP only.[9e] The onset potential (V_{onset}) of the acetate photooxidation was concentration-dependent and was ~ -1.4 V in 10^{-3} M TBAAc and ~ -1.6 V in 0.12 M TBAAc. Addition of acetic acid moved V_{onset} to more positive values, e.g., to ~ -1.4 V vs. Ag/0.1 N $AgNO_3$ (~ -1.05 V vs. SCE) for a solution containing 0.12 M of each TBAAc and HAc. Since the reduction of hydrogen ions could occur on Pt at these potentials, production of hydrogen at a Pt electrode short-circuited to an illuminated rutile electrode in a TBAAc/HAc mixture should be possible. The actual current measured through such a short-circuited electrode pair was about 200 $\mu A/cm^2$,[18] which was too small to lead to a significant rate of product evolution on the electrodes. This overlap of photooxidation and reduction ranges did however show important consequences for the heterogeneous photocatalytic decomposition of saturated carboxylic acids on TiO_2 powders.[19]

The height of the acetate photooxidation wave increased linearly with the concentration of TBAAc in the concentration range investigated (up to 0.12 M TBAAc) and approached the expected limiting photocurrent (for full lamp output) with 0.12 M TBAAc. At lower concentrations (but with the same light intensity) a plateau distinctly separated the photooxidation wave of acetate from the background oxidation (see Fig. 1[4]). As expected,[20] the light intensity also affected

both V_{onset} and photocurrent values for the acetate photooxidation. The c.v. current/potential curves (Fig. 1) generally had the following characteristics: (a) mass transfer-controlled behavior at low concentrations of TBAAc (e.g., 10^{-3} M) where the peak currents (i_p) varied with $v^{\frac{1}{2}}$, and the light intensity caused shifts of the peak potential (E_p) but had little effect on the peak current, or (b) a hole flux-controlled behavior at high concentrations of TBAAc (e.g., 0.12 M) where the cv i-V curve showed a plateau, i_p was independent of v, and i_p and E_p depended on the light intensity. E_p for case (a) was at -0.70 V vs. Ag/0.1 N $AgNO_3$ (for v = 1 V/sec and full output of lamp) with a half-peak potential, $E_{p/2}$, of -0.96 V, while for case (b) a half-wave potential of -1.07 V vs. Ag/0.1 N $AgNO_3$ with a voltammetric log slope (E vs. log $[(i_l-i)/i)]$) of about 200 mV was found (at 1% of full light output). Thus the oxidation of acetate on illuminated rutile occurred at about 2.0 to 2.3 V less positive potentials than on platinum electrodes, where a peak potential of +1.2 V vs. Ag/0.1 N $AgNO_3$ was found.[21] Chopping of the light at a frequency of 5 Hz[15] showed behavior characteristic of mass transfer control of the oxidation current at the plateau of the acetate oxidation wave (decay of current with time during the light periods) and established at the same time the absence of significant reduction currents in the dark periods. Finally, a wave length study showed the photooxidation of acetate on rutile electrodes (0.008 M TBAAc at 0.0 V vs. Ag/0.1 N $AgNO_3$) to be controlled by the light absorption characteristics of the semiconductor; the onset of the photooxidation was near 410 nm, with a quantum efficiency of ~ 0.85 at the maximum near 360 nm.

These results suggested the occurrence of an uncomplicated, heterogeneous, photoinduced Kolbe reaction, i.e., the one-electron oxidation of acetate (producing CO_2 and ethane). To check this hypothesis bulk electrolysis was performed with

mass spectral analysis of the gaseous reaction products, supported by gravimetric determination of CO_2 (as $BaCO_3$). The results of these experiments (described in ref. 4), showed that the normal Kolbe reaction (eq. 1) occurred readily at an illuminated rutile electrode at 0.0 V vs. Ag/0.1 N $AgNO_3$ in ACN containing TBAAc and HAc in comparable quantities. The mass spectrum showed ethane and CO_2 as the major gaseous products (a small amount of methane was also formed, ~ 5 - 10 vol. %, as the peak at m/e = 16 had two spikes and signals at m/e = 16, 15 and 14 exhibited the expected CH_4 distribution[4]). A quantitative (gravimetric) analysis for CO_2 in a similar experiment led to a current yield of CO_2 of 64%.

Acetate photooxidation in aqueous solutions. The occurrence of heterogeneous photodecarboxylation of acetate on illuminated TiO_2 powders[19] and the negative V_{fb} in ACN/acetate suggested studies of the photooxidation of aqueous solutions of acetic acid/sodium acetate mixtures on rutile electrodes. The effect of acetate on V_{fb}, as estimated from the onset potential of photooxidation, V_{onset}, was studied as a function of pH by using a constant total amount of acetate and changing the ratio of acetic acid to sodium acetate. The resulting values for V_{onset} paralleled the well-established 60 mV/pH-unit dependence of V_{fb} (Fig. 2). In the absence of oxygen these values agreed well with those obtained by open-circuit potential measurements. Moreover, the numerical values thus obtained were similar to those reported earlier from this[9f] and other laboratories.[9b,d,23,24] Thus, at a given pH, a significant change of V_{fb} upon addition of acetate/acetic acid does not occur. Nevertheless addition of acetate buffers does affect the rising portion of the anodic photocurrent observed on rutile electrodes by causing an easily recognizable wave to precede the solvent oxidation wave. At pH 6.75, high concentrations of acetate buffer ($\geq$ 0.1 M) cause the i-V curve to shift by about 200 mV towards more negative potentials without changing V_{onset} or the value of the limiting photocurrent (Fig. 3). Thus, as

with ACN, the ease of photooxidation of acetate results in a new photooxidation wave at more negative potentials. This is most pronounced with buffers sufficiently basic to contain a significant amount of free acetate; a 1 M acetic acid/sodium acetate buffer (100 : 1) results in only a 50 mV negative shift in the i-V curve. Because the presence of acetate buffers moved the photooxidation wave to more negative potentials, small, but noticeable, photooxidation currents could be seen at potentials where reduction of hydrogen ion occurred on a Pt-electrode (Fig. 4). Increasing the buffer concentration effected not only a shift of the photooxidation wave to more negative potentials, but also increased the magnitude of the hydrogen reduction current (half-wave potential at pH 3.5 ~ -0.48 V on Pt), so that high acetate buffer concentrations produced more favorable overlap of the two redox processes (Table 1). Consequently, short-circuiting an illuminated rutile electrode to a Pt-electrode[18] in the deoxygenated 1 M acetate-buffer solution (pH = 3.5, conditions as in Fig. 4) shifted the measured photopotential from the open-circuit-value of -0.41 to -0.30 (V vs. SCE) (a photocurrent of 43 $\mu A/cm^2$ flowed between the TiO_2 and Pt).

Because the acetate and water oxidation waves were not well separated, further analysis of the i-V curves was not undertaken, but again bulk electrolysis confirmed the importance of acetate photooxidation in acetate buffers. In an experimental setup similar to that described,[4] aqueous acetate buffers (5 M) at varying pH-values were photooxidized under N_2 on rutile electrodes, the evolved gases were swept through a solution of $Ba(OH)_2$ in 1 M NaOH, and the precipitated $BaCO_3$ was determined (Table 2). Generally, for each buffer two runs were done, one with the electrode potential set at the half-wave potential of the photooxidation wave and the other at +1.5 V, well into the limiting region. At both potentials, roughly the same overall current yield of CO_2 was obtained so that

the quantum yield was higher by a factor of about 2 for the more positive potential. The low current yields indicated co-oxidation of water and/or follow-up oxidations involving products derived from acetate oxidation. Indeed, mass spectral analysis of the gases produced during a photoelectrolysis of a deaerated 2 M acetate buffer (pH ~ 3.5) in 0.3 M $NaClO_4$ on a rutile electrode at 1 V vs. a Ag-wire quasi-reference revealed CO_2 and H_2 (from the reduction of acetic acid at the Pt-counterelectrode), and traces of ethane and methane, but oxygen was not found in significant amounts. No decomposition of the rutile electrode during electrolysis was noted.

Acetate photooxidation in acetic acid. We also investigated the photoelectrochemical behavior of rutile single crystal electrodes in water-free acetic acid solutions. In a solution containing 0.7 M $NaClO_4$ as electrolyte salt (high salt concentrations were used to ensure sufficient conductivity), no anodic faradaic current was observed in the dark in a potential range up to +9 V vs. the Hg/Hg_2Ac_2[16] electrode, while on the reductive side a broad cathodic wave at approximately -1.0 V with a limiting current density of ~ 400 $\mu A/cm^2$ was found. On Pt in this solution the oxidative cut-off occurred near +2.1 V and the reductive one near -0.6 V. Upon full illumination with the 450 W xenon lamp, a broad photooxidation wave appeared at potentials positive of -0.61 V vs. the Hg/Hg_2Ac_2 reference, gradually reaching a current plateau at potentials positive of +1 V, with a limiting current (~ 13 mA/cm^2) comparable to the values obtained in aqueous solutions (Fig. 5). Under these acidic conditions, the open circuit potential was -0.44 V and V_{onset} was -0.61 V. Controlled addition of sodium acetate led to a displacement of the onset potential, V_{onset}, to more negative values without affecting significantly the height of the photooxidation wave in the limiting current region (Fig. 6). The pH was calculated using the dissociation

constants[23] of sodium acetate (pK_6=6.56) and acetic acid (pK_s=14.45) and a regular shift of V_{onset} (~60 mV per pH-unit) was found. Similarly, addition of concentrated perchloric acid (70%) resulted in a shift in the opposite direction, again without a significant change in the limiting current in the positive potential regions. When the pH was calculated from the dissociation constant of perchloric acid in acetic acid (pK_a=4.87), V_{onset} was found to fall on the same potential/pH correlation obtained with NaAc in the higher pH-ranges. Thus, in water-free acetic acid a similar relation seems to hold between solution pH and flat band potential, V_{fb} (estimated as V_{onset}), of the rutile electrode, as found for aqueous solutions.[9b,d,f,22,24]

The high acid concentration in acetic acid solutions caused the hydrogen ion reduction to begin on the rutile electrode at potentials positive of V_{onset}, thus leading to open-circuit potentials - values significantly positive of V_{onset}. Pt electrodes showed a smaller overpotential for the reduction of hydrogen ions and for solutions of 0.01 M $HClO_4$/0.7 M $NaClO_4$ in HAc, a nearly reversible reduction wave of hydrogen ion on Pt was found at -0.44 V vs. Hg/$HgAc_2$. Therefore, the short-circuited electrode pair, consisting of an illuminated rutile electrode and a Pt-electrode[18] in HAc, 0.012 M NaAc, 0.8 M $NaClO_4$, showed a common potential (~-0.49 V) significantly positive of V_{onset} (-0.71 V); a short-circuit current of 68μA (170μA/cm^2) was observed (compare Fig. 1 in ref. 19a). Under the same conditions, an increase of the concentration of NaAc from 10^{-2} M to 1 M only slightly affected the short-circuit current (which increased from ~160 to ~240μA/cm^2), since both the onset of acetate photooxidation and the onset of hydrogen ion reduction were displaced to a similar degree. To check the effect of water on V_{onset} and on the proton reduction wave, water was added in controlled amounts to a 1 M solution of NaAc in HAc (up to 50% by volume). Again both waves moved to more negative potentials by similar amounts,

so that the photocurrent estimated to flow between a short-circuited electrode pair was nearly constant at ~100μA (~240μA/cm^2).

Discussion

The electrochemical behavior of n-type TiO_2 (rutile)-semiconductor electrodes has been well characterized in the dark and under illumination, in aqueous[8,9a-f,25-28] and in several non-aqueous solvents.[9e,17,26] Irradiation of light with a wavelength shorter than 410 nm (corresponding to the band gap energy E_g = 3.02 eV[6]) causes ejection of an electron from the valence band into the conduction band leaving behind a highly reactive valence band hole (h_v^+). This hole can subsequently be filled directly by an electron from a solution species, by an electron from an upper occupied semiconductor level (such as a surface state, an intermediate level or the conduction band itself) or cause oxidative photodecomposition of the semiconductor lattice. In aqueous solutions, photogenerated holes in n-TiO_2 materials are rapidly filled either by solvent oxidation or by competitive oxidation of an added oxidizable solution species,[9b,27] but photodecomposition of TiO_2 itself is not important, even at very high current densities.[28] The high current efficiency for photooxidation of halide, cyanide, sulfite, etc., (with increasing yield as the redox potential of the substrate becomes more negative), has been ascribed to the mediating action of surface states, situated about 1.3 V below the conduction band edge.[27] This conclusion was further corroborated by corresponding results in ACN as solvent.[9e] On the other hand, the photooxidation of water to yield O_2 has been shown recently not to be rate-limited by electrode kinetics but rather by the light flux, even at very high current densities.[28] This could be explained by a direct electron transfer via valence band holes as the primary step for

water oxidation (eq. 2); an isoenergetic process would be highly probable when the energy at the valence band edge ($E(h_v^+)$ = (3.07 - 0.059 pH)V), corresponds to the E° for the elementary step in the water oxidation reaction:[29]

$$(HO)_s + (H^+)_s + e^- \rightleftharpoons (H_2O)_s \quad (E° = (2.85 - 0.059\ pH)V)^{30} \qquad (2)$$

Similarly the photooxidation of acetate on n-type rutile electrodes probably occurs directly at the valence band itself (or very lowlying surface states), since the standard potential for acetate oxidation (eq. 3) has been estimated as +2.41 V.[31]

$$CH_3CO_2^{\cdot} + e^- \rightleftharpoons CH_3CO_2^- \quad E° = +2.41\ V \qquad (3)$$

Moreover, the pH-dependence of the standard potential in (2) and of the energy of the valence band edge should lead to a significant pH-dependence in the competition between water oxidation and acetate oxidation, assuming the latter reaction is not significantly affected by pH at pH-values near pK_a (HAc) or higher. Correspondingly, on Pt-electrodes the electrooxidation of aqueous acetate solutions has to be performed at highly positive potentials (E > 2.2V), with high current densities and at low pH-values, to suppress water oxidation.

The data presented here (Table 2) tend to support a pH-dependent competition of acetate and water for hole capture in rutile electrodes. The comparatively high current yields for CO_2 formation from acetate oxidation in the pH-range investigated (assuming water oxidation is the only complementary process) indicate a high relative reactivity for acetate, especially at the lower pH-values. Similarly, the related photocatalytic decarboxylation of aqueous HAc/NaAc mixtures on n-type TiO_2 powder (anatase) revealed a considerable pH-dependence (with decreasing absolute yield of decarboxylation at high and very low pH-values),[19b] in this case however the effect of pH on the reduction of oxygen and the adsorption of acetate might also play a role.

The high reactivity of acetate for capturing the photogenerated holes also causes a significant displacement of the photooxidation wave to more negative potentials upon addition of acetate buffer to an aqueous solution of appropriate pH. Analysis of the foot of the oxidation wave reveals no significant change of the potential for the onset of photooxidation ($V_{onset} \simeq V_{fb}$), but the rise of the photocurrent (with potential) is steeper in the presence of acetate. Therefore acetate oxidation competes favorably with internal electron-hole recombination within the semiconductor, even at potentials near V_{fb}. An important factor in the efficient oxidation of acetate is the absence of a back reduction of oxidized species; the final products of a Kolbe reaction, i.e., acetate, CO_2, and ethane (and side products, e.g., methane, methanol, etc.), are not reduced in the dark in this potential region. On the other hand, the stable end product of water photooxidation, oxygen, can be reduced on rutile at potentials even positive of V_{fb}, so that an external recombination mechanism for the electron-hole pair of the semiconductor exists. This "short-circuiting" oxidation-reduction cycle will yield no net current until the potential is sufficiently positive to prevent the back-reduction of photogenerated oxygen. This effect is particularly important at the foot of the photooxidation wave. To amplify further this effect, we studied the dark reduction of oxygen on rutile electrodes in the pH-range of acetate buffers. As illustrated in Fig. 8, at pH = 3.4 the reduction wave of oxygen occurs at potentials considerably positive of V_{fb}. Moreover, it is in the same potential region that with the chopped mode of illumination at 5 Hz sharp current spikes are seen whenever the illuminated state changes. These reductive and oxidative current spikes are significant only in potential regions where both photooxidation of water and reduction of oxygen occur to a significant extent (Fig. 8). Note also that

oxygen saturation of an aqueous acetate buffer (0.1 M HAc, 5.6 mM NaAc) depressed the open-circuit photopotential, V_{oc}, of a rutile electrode from -0.40 to -0.31 V vs. SCE; V_{oc} represents the potential where oxygen reduction and photooxidation occur at equal rates. Thus the displacement of the photooxidation wave in the presence of acetate to more negative potentials can be attributed to two effects which enhance the overall efficiency for photooxidation near V_{fb}: the high reactivity of acetate with the photogenerated holes and the absence of significant reduction of photooxidation products.

Similarly the reduction of hydrogen ions in the aqueous acetate buffers investigated occurs at potentials positive of V_{fb}. Although this effect is only barely discernible on the rutile electrode (because of the sluggish reduction of acid on this material), on a Pt-electrode a considerable reduction current can be observed at V_{onset} in deaereated aqueous acetate buffers (Fig. 4). As illustrated in Table 1, this leads to an increasing current at an illuminated rutile electrode short-circuited to a Pt-cathode with increasing acetate buffer concentration. Similarly, as with oxygen, the open-circuit photopotential of a TiO_2-Pt-electrode pair[18] is shifted positively from V_{oc} of the TiO_2 electrode alone. Again the reduction process occurring at the metal electrode lowers the Fermi level in the electrode pair to a potential positive of V_{fb}. Cyclic voltammetry on a Pt-disk electrode shows a nearly reversible reduction wave (at buffer concentrations $\leq$ 0.1 M, HAc : NaAc = 18 : 1, pH = 3.5) at a potential of ~-0.48 V vs. SCE (E_{pc} = -0.53, E_{pa} = -0.45 V) attributed to reduction of hydrogen ions to molecular hydrogen. Thus the foot of the hydrogen ion reduction wave extends well into the region positive of V_{fb} (with an increasing effect as the concentration of buffer increases); part of the reductive current on Pt or TiO_2 positive of V_{fb} may also result from the reduction to adsorbed hydrogen.

Substitution of acetic acid for water as solvent leads to results qualitatively similar to those in aqueous buffers with an even more pronounced overlap of the potential regions for reduction of hydrogen ion and photooxidation of acetate on rutile electrodes. Thus, the largest current densities for the TiO_2 - Pt electrode pair were found for sodium acetate solutions in acetic acid. Accompanying studies of the dependence of V_{fb} of rutile electrodes (estimated from V_{onset}) with solution pH in acetic acid revealed the same linear correlation between pH and V_{fb} as had previously been found for rutile in aqueous solutions. In acetic acid, the acid/base pairs $(H^+)_{HAc}$/HAc and HAc/$(Ac^-)_{HAc}$ seem to play the same role as the one ascribed to the aqueous species $(H^+)_{H_2O}$/H_2O and $H_2O/(OH^-)_{H_2O}$ in water,[22,30] i.e., they induce protonation - deprotonation equilibria of semiconductor surface, resulting in a displacement of V_{fb} by 59 mV per pH-unit. A qualitatively similar effect was also observed in acetonitrile solution where increasing the concentration of TBAAc caused a negative shift of V_{onset}, while subsequent addition of HAc moved V_{onset} back to more positive potentials.

Only in acetonitrile is the photooxidation wave of acetate clearly set apart from the background photooxidation, which starts about 1.3 to 1.5 V positive of V_{fb}, (near the energy ascribed to an intermediate level or a surface state of a rutile single crystal electrode[9e]). One can speculate, as was done in a model previously proposed,[15] that this intermediate level mediates recombination of the photogenerated electron-hole pairs and that only when the potential is sufficiently positive to prevent filling of this level from the conduction band will the slow photooxidation of a solution species proceed at an appreciable rate in the absence of acetate. Addition of easily photooxidizable acetate (as TBAAc) causes the photogenerated holes to be intercepted

at a very low energy level, probably at the valence band edge itself. Therefore, only weak bending of the bands positive of V_{fb} leads to significant photooxidation of acetate. In absence of mass transfer control, the half-wave potential of the photooxidation wave for acetate in ACN is situated about 2.3 V negative of where the corresponding half-wave potential on Pt was measured. Under mass transfer-controlled conditions (low acetate concentration) the corresponding peak potentials developed in a cyclic voltagramm showed a somewhat smaller displacement (~2 V). Thus in ACN solution, more than 2/3 of the band gap energy is utilized in the photocatalytic step, where the oxidation is promoted by at least 2.0 to 2.3 V. Similar, slightly smaller underpotential or negative overpotential-values are found with acetic acid and water as solvents; e.g. at a current density of 2 mA/cm^2 acetate oxidation occurs at -0.2 V on illuminated rutile vs. +1.5 V on Pt for 1 M NaAc in HAc. Preparative experiments involving bulk electrolysis of acetate in ACN on illuminated rutile electrodes at potentials corresponding to considerable underpotentials showed the photooxidation of acetate to follow the normal course of a Kolbe reaction (eq. 1) leading to high yields of carbon dioxide and ethane as the main products. In aqueous solution the photocatalyzed decarboxylation of acetate is accompanied by side reactions (probably the oxidation of water) so that CO_2 is formed with lower current yields and the formation of ethane is also low.

The results presented here also pertain to those obtained in the heterogeneous photocatalytic decarboxylation of saturated carboxylic acids on TiO_2-powders.[19] There photodecomposition gave alkanes and CO_2 in a photoassisted oxidation-reduction cycle occurring on the powder-surface (with the light energy bridging the overpotential gap between oxidation of carboxylate and reduction of carboxylic acids). Contrasting the results obtained on the rutile electrodes however, the product of acetate decarboxylation on the powder platinized

antase catalysts was mainly methane (and CO_2). Our interpretation ascribed this mainly to the large surface area of the powders, resulting in only small surface concentrations of intermediate radicals as well as the location of reductive sites near those where the methyl radicals are produced. Basically, however, the essential features governing the oxygen-free decomposition of saturated carboxylic acids on these powders also evolves from the measurements on rutile single crystal electrodes reported here, i.e., a short-circuited illuminated rutile/Pt-electrode pair, promotes the photooxidation of carboxylates (on the semiconductor) with concominant reduction of hydrogen ions on the metal electrode, resembling the local cell process occurring on the (partially metallized) powder particles.[19]

Acknowledgments

The support of this research by the Schweizerische Nationalfonds zur Foerderung der wissenchaftlichen Forschung (to B.K.) and by the National Science Foundation and the Robert A. Welch Foundation is gratefully acknowledged.

References and Notes

1. A. Heller (ed.) "Semiconductor Liquid-Junction Solar Cells," Proceedings Vol. 77-3, The Electrochemical Society, Princeton, N.J., 1977 and references therein.

2. S. N. Frank & A. J. Bard, J.Am.Chem.Soc., 99, 303 (1977); S. N. Frank & A. J. Bard, J. Phys. Chem., 81, 1484 (1977).

3a. H. Kolbe, Ann. Chem., 69, 257 (1849);

b. see e.g. I.H.P. Utley in N.L. Weissberger (ed.), "Technique of Electro-organic Synthesis," Vol.I, p.793, Wiley Interscience, New York, N.Y., 1974; L. Eberson in S. Patai (ed.), "The Chemistry of Carboxylic Acids and Esters," p. 53, Interscience Publishers, London, 1969; L. Eberson in M.M. Baizer (ed.), "Organic Electrochemistry," M. Dekker, New York, N.Y., 1973.

4. B. Kraeutler & A. J. Bard, J. Am. Chem. Soc., 99, 7729 (1977). The light energy therefore is used only in a catalytic sense.

5. In the gas phase the half lifetime of the acetoxy radical at 65° is 10^{-10} sec; W. Braun, L.Rajbenbach & F.R. Eirich, J. Phys. Chem., 66, 1591 (1962).

6. V.N. Pak & N.G. Ventov, Russ. J. Phys. Chem., 49, 1489 (1975).

7a. H. Gerischer, J. Electroanal. Chem., 82, 133 (1977);

b. A.J. Bard & M.S. Wrighton, J. Electrochem. Soc., 124, 1906 (1977).

8. M.S. Wrighton, D.S. Ginley, P.T. Wolczanski, A.B. Ellis, D.L. Morse & A. Linz, Proc. Nat. Acad. Sci. USA, 72, 1518 (1975).

9a. A. Fujishima & K. Honda, Bull. Chem. Soc. Jap., 44, 1148 (1971);

b. E.C. Dutoit, F. Cardon & W.P. Gomes, Ber. Busenges., 80, 1285 (1976);

c. L.A. Harris & R.H. Wilson, J. Electrochem. Soc., 123, 1010 (1976);

d. J.M. Bolts & M.S. Wrighton, J. Phys. Chem., 80, 2641 (1976);

e. S.N. Frank & A.J. Bard, J. Am. Chem. Soc., 97, 7427 (1975);

f. K.L. Hardee & A.J. Bard, J. Electrochem. Soc., 122, 739 (1975); ibid., 124, 215 (1977).

10. H. Gerischer & H. Roessler, Chem.-Ing. Tech., 42, 176 (1970).

11. S.N. Frank, A.J. Bard & A. Ledwith, J. Electrochem. Soc., 122, 898 (1975).

12. R. Noufi, P.A. Kohl, S.N. Frank & A.J. Bard, J. Electrochem. Soc., 125, 246 (1978).

13. A. Fujishima, K. Honda & S. Kicuchi, J. Chem. Soc. Jap., 72, 108 (1969).

14. C.K. Mann in A.J. Bard (ed.), "Electroanalytical Chemistry," Vol. III, p. 57, M.Dekker, New York, N.Y., 1969.

15. P.A. Kohl & A.J. Bard, J. Am. Chem. Soc., 99, 7531 (1977).

16. W.B. Mather & F.C. Anson, Anal. Chim. Acta, 21, 468 (1959).

17. K. Nakatani & H.Tsubomura, Bull. Chem. Soc. Jap., 50, 783 (1977).

18. The Pt-electrode had a surface of ~ 20 cm^{-2}; the current densities are given for the illuminated semiconductor, area 0.4 - 0.5 cm^{-2}.

19a. B. Kraeutler & A.J. Bard, J. Am. Chem. Soc., 100, 2239 (1978).

b. B. Kraeutler & A.J. Bard, J. Am. Chem. Soc., (in press).

20. H. Gerischer, J. Electroanalyt. Chem., 58 263 (1975).

21. D.H. Geske, J. Electroanal. Chem., 1, 502 (1959/60) reported a halfwave potential of +1.58 - 1.63 V vs. SCE under similar conditions.

22. T. Watanabe, A. Fujishima, O.Tatsuoki & K. Honda, Bull. Chem. Soc. Jap., 49, 8 (1976).

23. A.I. Popov in J.J. Lagowski (ed.), "The Chemistry of Nonaqueous Solvents," Vol. III, p. 241, Acad. Press, New York, N.Y., 1970.

24. W.K.K. Clark & N. Sutin, J. Am. Chem. Soc., 99, 4676 (1977).

25. T. Ohnishi, Y. Nakato & H. Tsubomura, Ber. Bunsenges., 79, 523 (1975).

26. M. Miyake, H. Yoneyama & H. Tamura, Denki Kagaku, 45, 411 (1977).

27. S.N. Frank & A.J. Bard, J. Am. Chem. Soc., 99, 4667 (1977).

28. A.B. Bocarsly, J.M. Bolts, P.G. Cummins & M.S. Wrighton, Appl. Phys. Lett., 31, 568 (1977).

29. H. Gerischer in H. Eyring, D.Henderson & W. Jost (eds.), "Physical Chemistry, an Advanced Treatise," Vol.IXA, Acad. Press, New York, N.Y., 1970.

30. E. Yeager, in "Electrocatalysis on Non-Metallic Surfaces," NBS Special Publication 455, Gaithersburg, Md., Dec. 9-12, 1975 (Issued Nov. 1976).

31. L. Eberson, Acta. Chim. Scand., 17, 2004 (1963); this value was derived for a free solution process.

Table 1 Effect of total buffer concentration (HAc:NaAc = 18 : 1) on onset potential, open-circuit potentials and zero bias photocurrents of an illuminated rutile single crystal electrode in aqueous acetate buffer[a]

conc.	V_{onset}[b]	$V_{oc}(TiO_2)$[b]	$V_{oc}(TiO_2\text{-}Pt)$[b,c]	$i(TiO_2\text{-}Pt)$[c]	i_o[d]
10^{-2} M	-0.40	-0.39	-0.36	2	5
10^{-1} M	-0.41	-0.40	-0.34	4	10
1 M	-0.42	-0.41	-0.30	17	43
10 M	-0.43	-0.42	-0.22	56	140

a) The solution was 1 M $NaClO_4$; and indicated total acetate concentration. Electrode was irradiated with full output of 450 W Xe lamp.

b) V vs. SCE.

c) Rutile electrode short-circuited to Pt-electrode, in μA.[18]

d) $\mu A/cm^2$, at zero bias between electrodes.[18]

Table 2 Evolution of CO_2 on illuminated rutile electrode; bulk electrolysis of aqueous acetate buffer solutions.[a]

pH	Applied potential (V vs. SCE)	$BaCO_3$ produced (mg)	Current efficiency[b]	Quantum efficiency[c]	log.Φ[d]
2.7	0.15	26.5	0.32	0.13	3.02
2.7	1.5	28.5	0.24	0.19	2.88
3.4	0.08	37	0.27	0.11	2.22
3.4	1.5	96	0.32	0.25	2.32
4.8[e]	0.0	37	0.25	0.10	1.05
6.8	-0.12	20	0.19	0.08	0.44
6.8	1.5	18	0.17	0.14	0.40
9[f]	1.5	11.5	0.15	0.12	0.26

a) full output 450 W Xenon lamp.

b) from rate of CO_2 evolution and total current.

c) estimated from amount of CO_2 evolved and assuming total limiting photocurrent corresponds to a quantum yield 0.8 for light greater than the rutile band-gap.

d) Φ = rel. hole reactivity for acetate vs. water; defined as

$$\Phi = \frac{\text{curr. eff.}}{1 - \text{curr. eff.}} \cdot \frac{\text{acetate conc.}}{\text{water conc.}}$$

e) 3 M buffer.

f) 5 M NaAc.

Figure Captions

Fig. 1.a. Mass transfer controlled photooxidation wave of acetate in ACN on rutile s.c. electrode: 0.001 M TBAAc in ACN/0.1 M TBAP; scan rate 1 V/sec; full intensity of 450 W Xe lamp.

b. Lightflux controlled photooxidation wave of acetate in ANC on rutile s.c. electrode: 0.12 M TBAAc in ACN/0.1 M TBAP; scan rate 0.5 V/sec; 1% of full light intensity of 450 W Xe lamp.

Fig. 2. pH-dependence of the onset potential of photooxidation (V_{onset}) of various acetate-buffers (total acetate concentration 1 M) in 4 M aqueous $NaClO_4$ solutions on a rutile s.c. electrode: circles: exptl. results; full line has theoretical slope of 59 mV/pH, broken lines are flat band potential vs. pH relationships taken from (a) Fujishima et. al. (ref. 22) and (b) from Dutoit et. al. (ref. 9b).

Fig. 3. Photocurrent vs. potential curves on an illuminated rutile s.c. electrode for aqueous acetate buffers (NaAc : HAc = 100 : 1 ; pH 6.7) in 0.5 M $NaSO_4$ solutions with varying total acetate buffer concentrations: 1 = 0.001 M; 2 = 0.01 M; 3 = 0.1 M; 4 = 1 M.

Fig. 4. Current potential curves in aqueous 1 M $NaClO_4$ containing 1 M acetate buffer (HAc : NaAc = 18 : 1).

Fig. 5. Current potential curves in HAc/0.7 M $NaClO_4$ (rutile s.c. electrode, 450 W Xe lamp, Pt disc electrode).

Fig. 6. Calculated pH-dependence of the onset potential of photooxidation (V_{onset}) on a rutile s.c. electrode of acetic acid solutions containing NaAc (0.001, 0.01, 0.1, and 1 M; open circles) and $HClO_4$ (0.01, 0.1 and 1 M; full circles) and 0.7 M $NaClO_4$ based on the dissociation constants of HAc, NaAc and $HClO_4$ in acetic acid, ref. 23.

Fig. 7. Estimated potential relationships (with respect to NHE) on a rutile electrode immersed into aqueous acetate solutions at pH 5 (illustrated at an applied potential of +0.2 V vs. NHE).

Fig. 8. Current potential curves showing oxygen reduction in an oxygen saturated aqueous 0.1 M acetate buffer at pH 3.4.

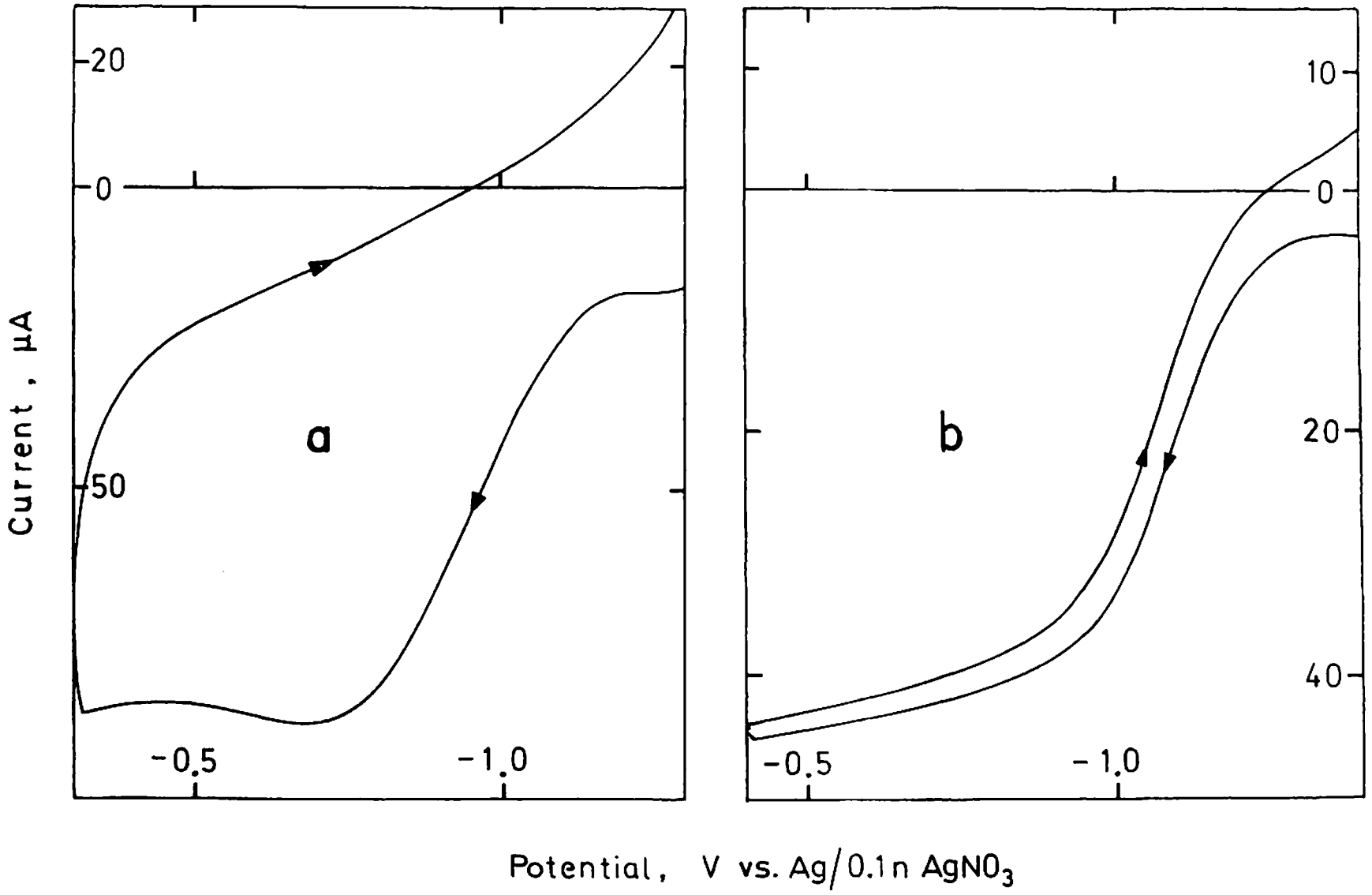
20
0
50
a
-0.5
-1.0
10
0
20
40
b
-0.5
-1.0
Current, μA
Potential, V vs. Ag/0.1n AgNO3

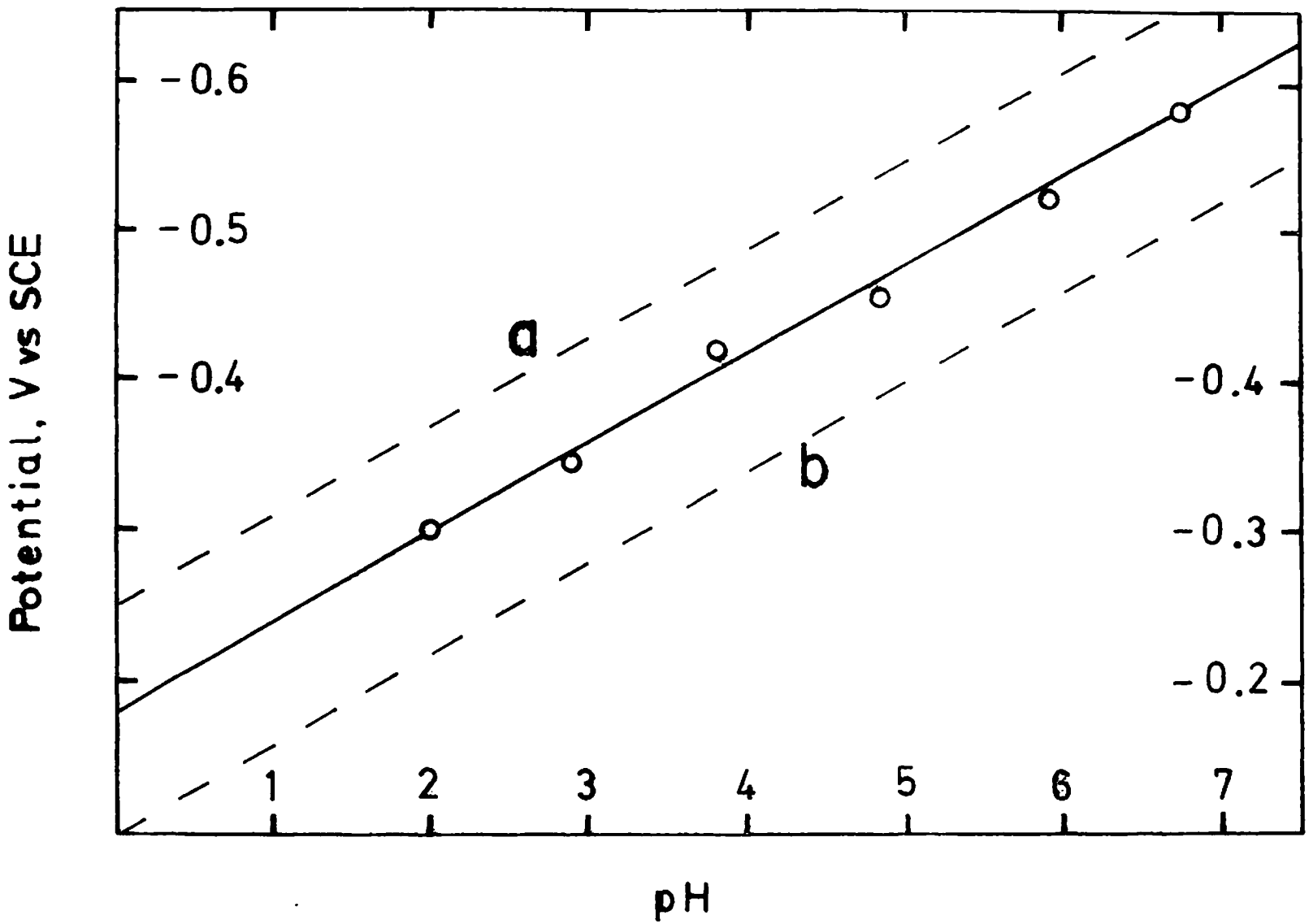

Fig 2

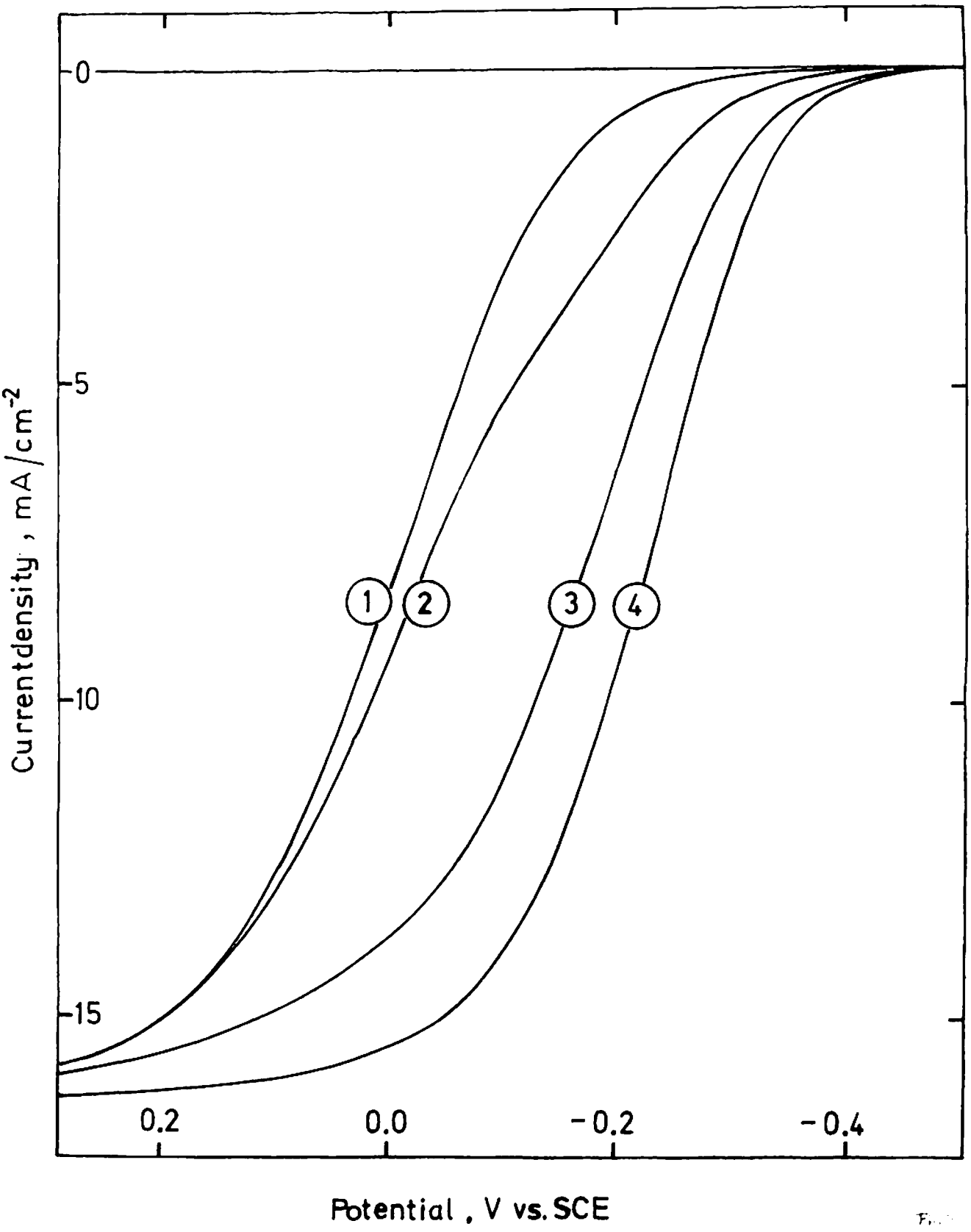
0
-5
-10
-15
Currentdensity , mA/cm-2
1
2
3
4
0.2
0.0
-0.2
-0.4
Potential , V vs. SCE

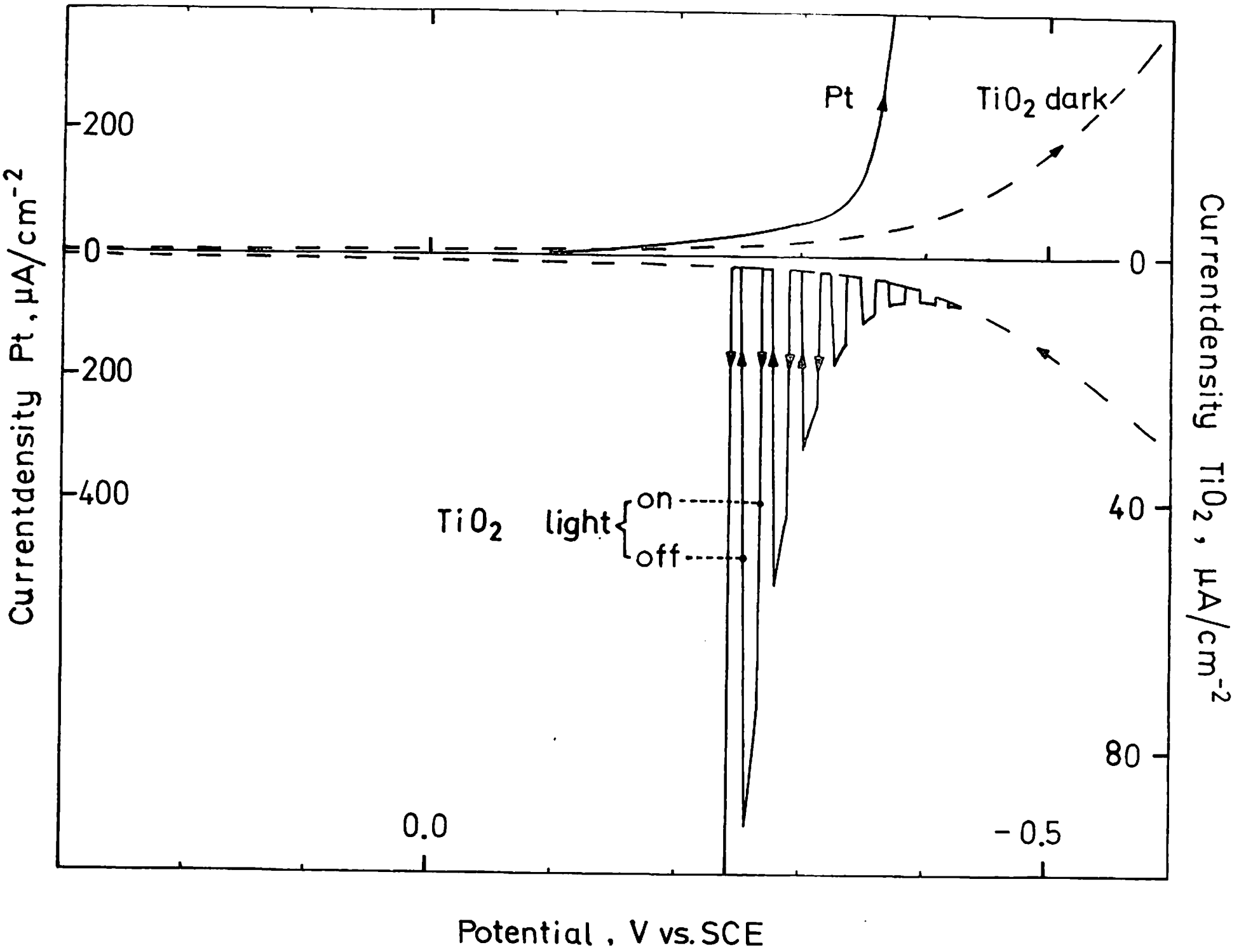
Pt
TiO2 dark
200
0
200
400
TiO2 light
on
off
0.0
-0.5
0
40
80
Currentdensity Pt, μA/cm-2
Currentdensity TiO2, μA/cm-2
Potential, V vs. SCE

Fig. 4

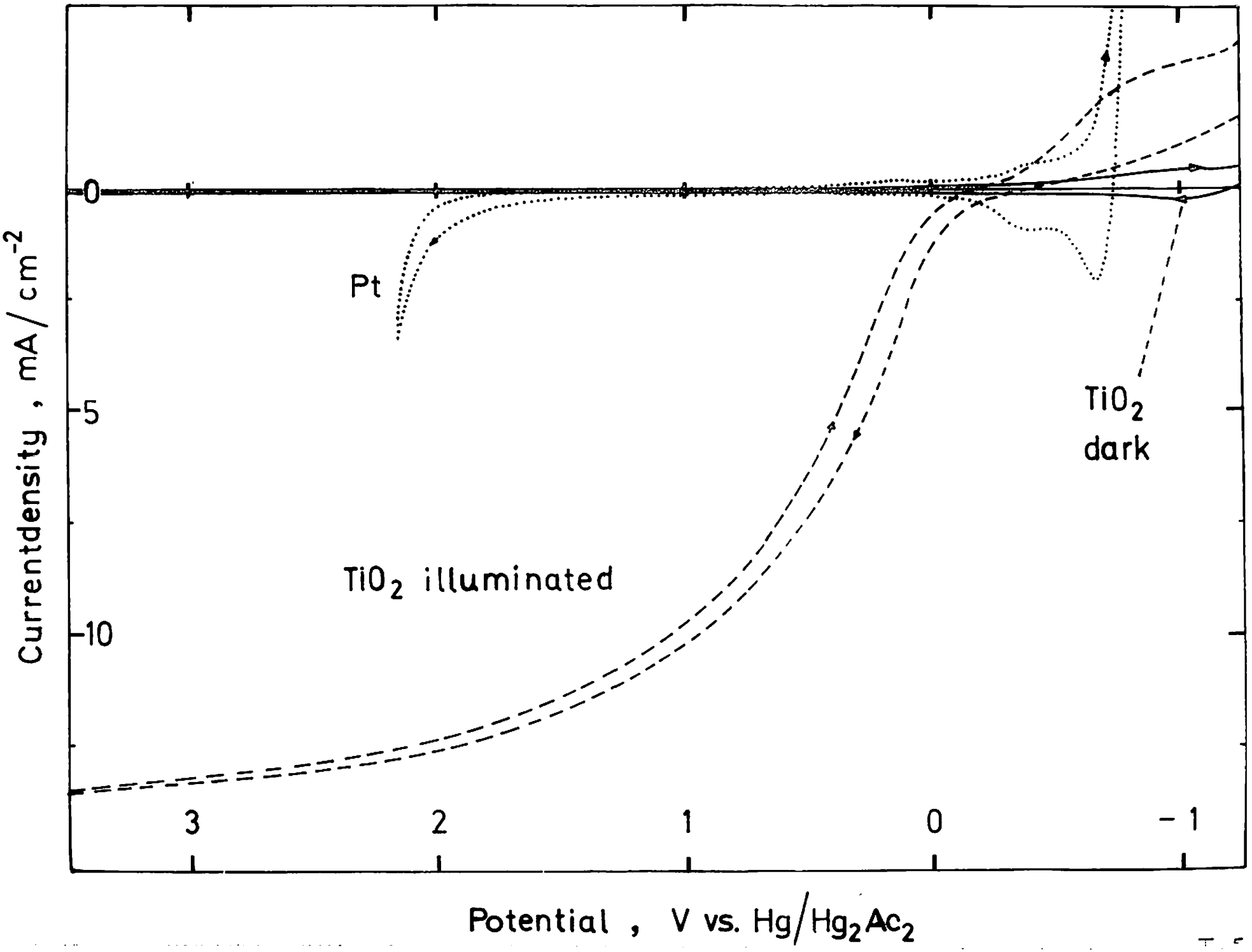
0
-5
-10
Currentdensity , mA / cm^{-2}
Pt
TiO_2 illuminated
TiO_2 dark
3
2
1
0
-1
Potential , V vs. Hg/Hg_2Ac_2

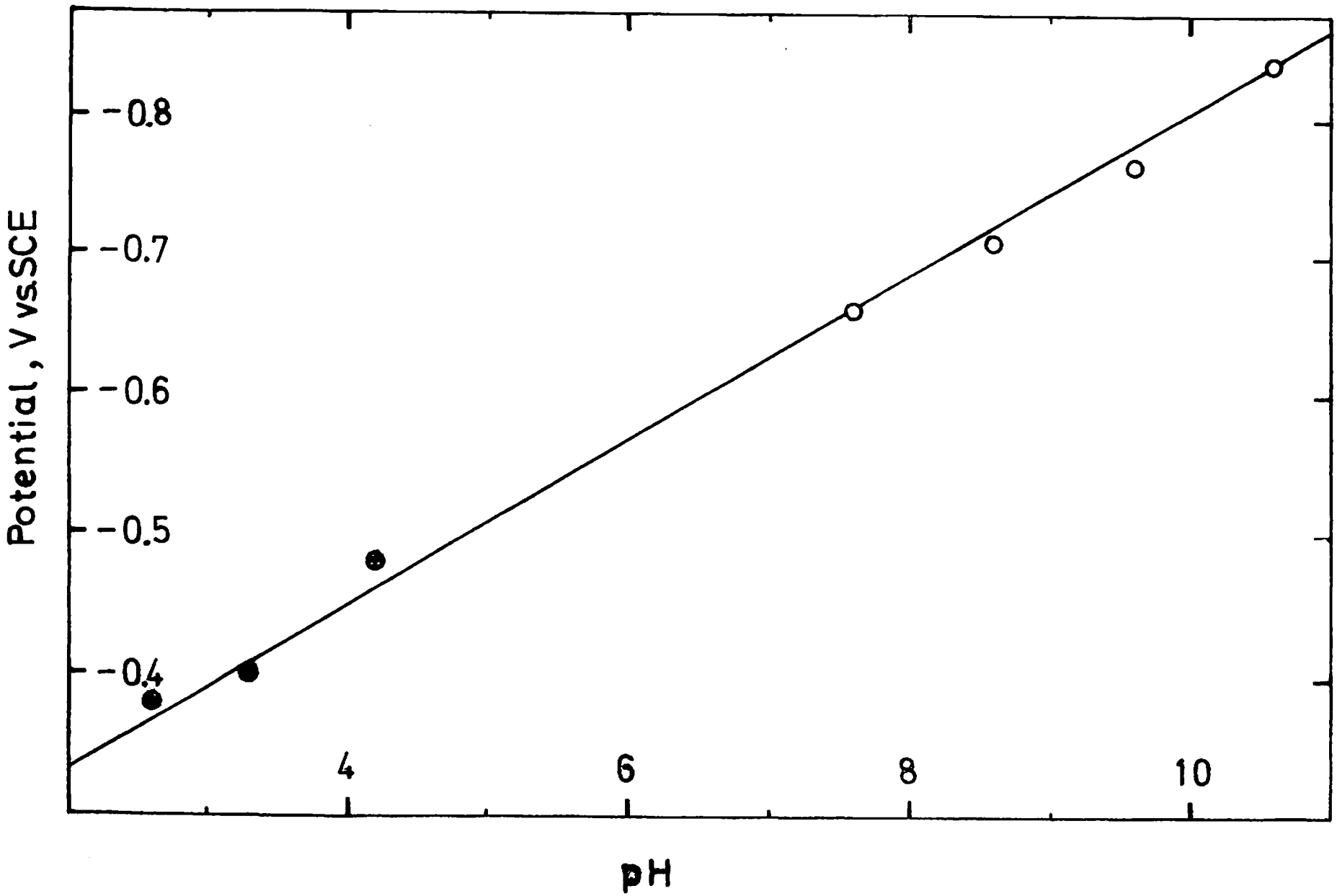

Fig 6

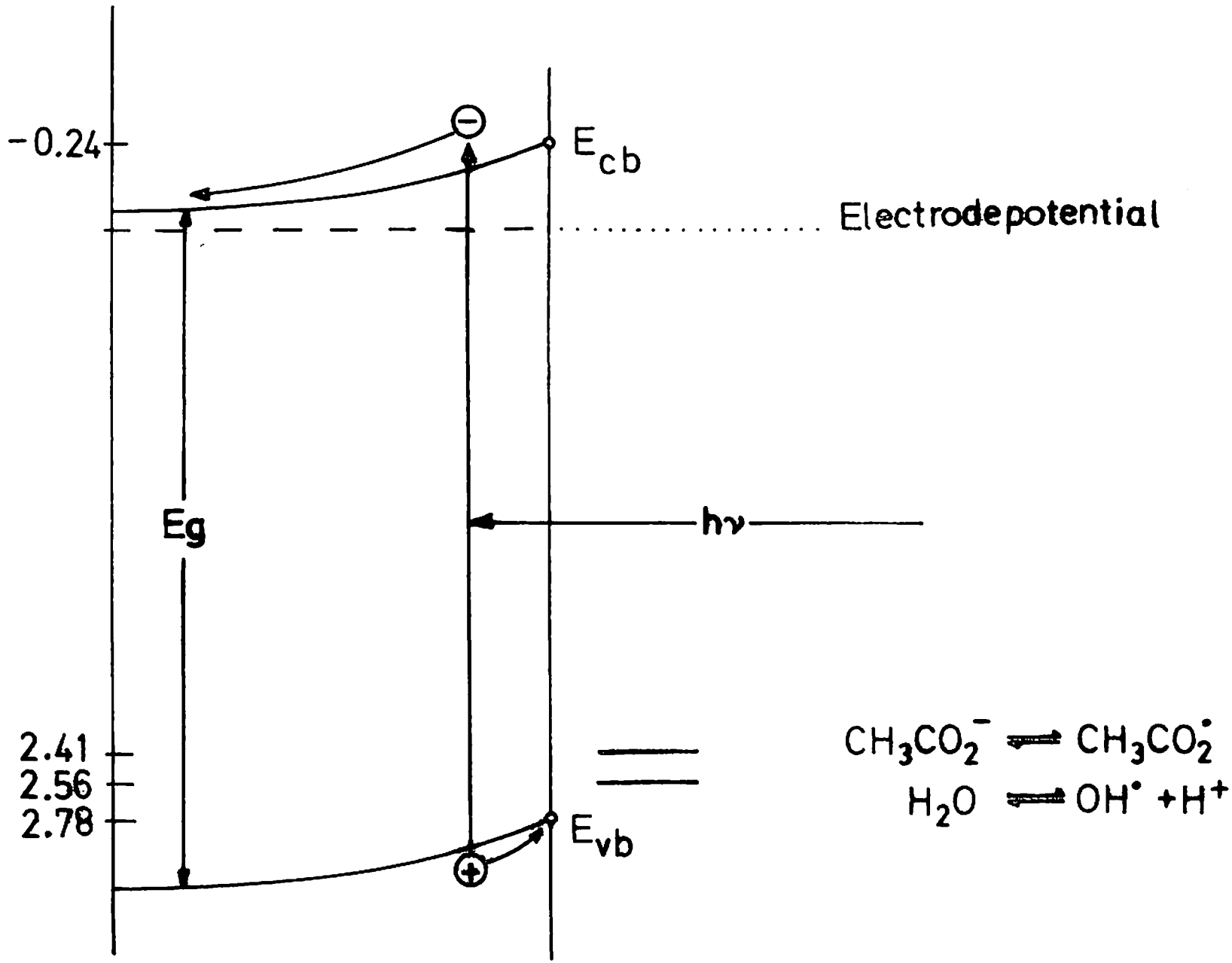
-0.24
E_{cb}
Electrodepotential
Eg
hν
2.41
2.56
2.78
E_{vb}
$CH_3CO_2^- \rightleftharpoons CH_3CO_2^{\bullet}$
$H_2O \rightleftharpoons OH^{\bullet} + H^+$

Fig 7

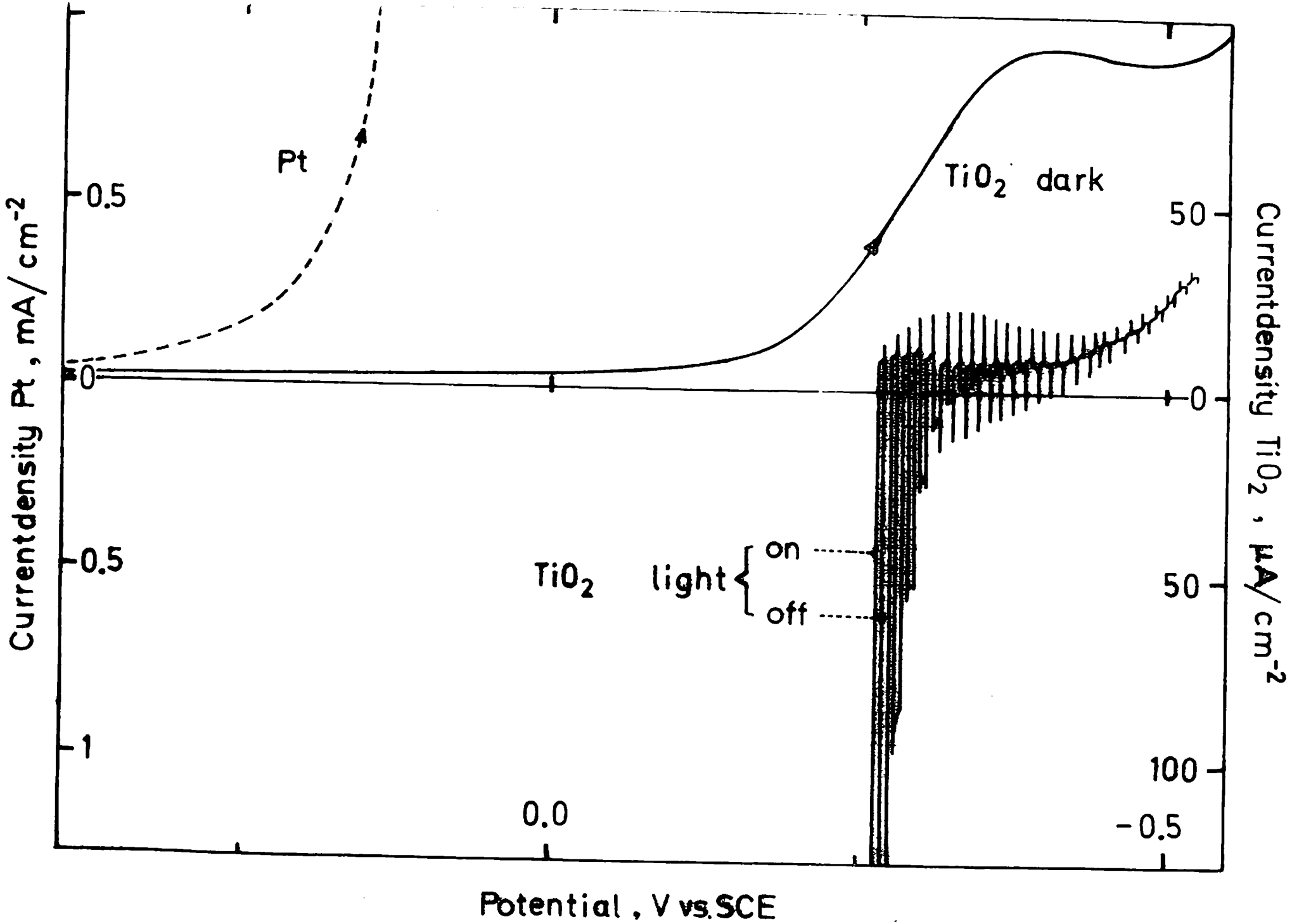
Pt
TiO2 dark
TiO2 light
on
off
0.5
0
0.5
1
0.0
50
0
50
100
-0.5
Currentdensity Pt , mA/cm-2
Currentdensity TiO2 , µA/cm-2
Potential , V vs.SCE